Hindawi
Journal of Advanced Transportation
Volume 2022, Article ID 5458115, 14 pages
https://doi.org/10.1155/2022/5458115

Research Article

Transit Signal Priority for an Integrated Traffic Signal System

Minji Kim, Yohee Han, and Youngchan Kim

Department of Transportation Engineering, University of Seoul, Seoul 02504, Republic of Korea

Correspondence should be addressed to Yohee Han; yeohee@gmail.com

Received 5 May 2022; Revised 6 August 2022; Accepted 7 September 2022; Published 17 September 2022

Academic Editor: Ruimin Li

Passive transit-signal priority (TSP) is an effective approach to improve the operational efficiency of transit systems on arterial roads. This paper presents an integrated TSP model that benefits both transit vehicles and other road users. The proposed model uses the random arrival characteristics of transit vehicles related to their stochastic dwell times at near-side stops. Thus, it enables not only two-way bandwidth maximization within subsystems but also the combined optimization of adjacent subsystems. To minimize any negative impact on side-street traffic, this study, unlike previous research, considers the influential area by the introduction of TSP. Case studies on 15 intersections in Sejong, Korea, verify the superior performance of the proposed model for both transit and general vehicles.

1. Introduction

Transit-signal priority (TSP) is the most efficient method of ensuring the rapidity of transit vehicles on an arterial road network. Most prior research on TSP has involved expanding the general-vehicle arterial signal-coordination model. Although various effective TSP models have appeared in the literature, TSP control has been rarely applied in practice because of concerns over its negative impact on non-transit road users. Thus, progression models that can benefit both general and transit vehicles are of considerable interest.

Over the past few decades, several researchers have proposed optimization approaches for arterial signal progression. Brooks [1] suggested optimizing arterial bandwidth through half-integer synchronization, considering only two through phases. Messer et al. [2] extended Brooks' model to a multiphase-signal case. Subsequently, Little and Kelson [3] designed MAXBAND, which maximizes a weighted combination of bandwidths, including the optimal cycle length, offsets, speeds, and order of left-turn phases. However, MAXBAND can only be used to optimize signal timing plans for arterials. Chang et al. [4] overcame this limitation with MAXBAND-86, which can determine the global optimum solution for a large signal network. Gartner et al. [5] developed MULTIBAND, which considers the actual traffic volumes and flow capacities of each link, generating an individually weighted bandwidth for each road direction.

On the basis of these earlier models, Tian and Urbanik [6] proposed a system-partition technique that maximizes the bandwidth in the peak direction and provides partial progression for the off-peak traffic period. Lin et al. [7] developed a new mixed-integer nonlinear programming model that maximizes the number of intersections that can be passed without stopping; although suitable for high-saturation traffic conditions, it calculates the long cycle length under low-saturation ones. Li [8] solved the progression time uncertainty using MAXBAND and Monte Carlo methods, considering the mean bandwidth, standard deviation, and minimum bandwidth by varying the cycle-by-cycle period. Yang et al. [9] reported three multipath progression models that overcome the limitations of existing models maximizing only two-way bandwidth or minimizing their total delay. Zhang et al. [10] proposed Asymmetrical MULTIBAND (AM-BAND), which relaxes the requirements of MULTIBAND and utilizes the green times in each direction more appropriately. Ye et al. [11] developed a two-way bandwidth maximization model considering the queue-clearance time, which had been neglected in previous studies. Zhang et al. [12] designed MaxBandLA, which maximizes the mean two-way bandwidth and produces an optimal network partition plan, and MaxBandGN, which

optimizes the offsets for all the signals in a grid network. Yang and Cheng [13] developed geometry-based signal-optimization models for asymmetric continuous-flow intersections. Hao et al. [14] discussed the maximal number of subgroups for effective signal progression when a long arterial contains several intersections.

To improve the efficiency of transit-signal operation in terms of progression control, Ma et al. [15] developed a person-capacity-based optimization method using a binary mixed-integer linear program. This model can be used to produce optimal lane markings, exclusive bus lanes, and TSP signal timings for isolated intersections; however, it imposes a spatial limit as a transit vehicle travels along the arterial road. Jeong and Kim [16] designed TRAMBAND, which can find the maximized general-vehicle bandwidth for a fixed tram bandwidth along the arterial using MAXBAND. However, the MAXBAND model with equal bandwidths at multiple sections limits green-time-utilization efficiency. Bai et al. [17] proposed TRAMBAND, employing AM-BAND for more efficient use of the green time. In a similar context, Florek [18] reported the BUS-MULTIBAND and BUS-AM-BAND methods, which solve the signal-coordination problem for passenger cars and public-transport vehicles simultaneously. Dai et al. [19] and Ma et al. [20] addressed the competing demands of transit and general vehicles by constraining the minimum bandwidth. Dai et al. [21] categorized the intersections along the main street based on bus-stop locations and optimized signal coordination to consider the bus speed and dwell time. To enhance the passive control strategy under dwell-time uncertainty, Kim et al. [22] developed bus-based signal coordination, which account for the average dwell time and its variance on arterial roads with heavy bus volumes. Han et al. [23] designed STEP BAND, a progression-control-based TSP that follows a uniform arrival distribution. STEP BAND supports nonstop bus movement and reduces delays for general vehicles driving on the main road.

In addition, active strategies can be used to give priority to specific transit vehicles [24]. Garrow and Machemehl [25] described and evaluated several TSP-provision methods during both peak and off-peak periods. The results indicated that active TSP should be used cautiously during peak periods. Several other studies have been conducted to improve transit systems using active TSP [26–30]. However, the negative effect of active TSP strategies (especially that of nonpriority phases) on general traffic has elicited concern [31]. Therefore, Kim et al. [32] developed a bus-oriented base signal plan for an arterial road, activating TSP only at critical intersections.

The contributions of the present study are twofold: first, we attempt to maximize the two-way bus bandwidth within the subsystem and optimize the combination of adjacent subsystems by considering bus-bay capacity and a random bus-arrival distribution based on the stochastic dwell time at a near-side bus stop. Second, the influential area by TSP, ignored in previous studies, is included in the optimization. The remainder of this paper is organized as follows: a detailed statement of the problem is presented in Section 2. The proposed methodology is discussed in Section 3, and the test site is described in Section 4. In Section 5, the performance and effectiveness of the proposed model are compared with those of existing signal systems. The conclusions of this study are presented in Section 6.

2. Problem Definition

Passive TSP is a strategy to establish signal progression for transit by varying split length, offset, and cycle length [24, 33]. This strategy can be implemented by manually modifying the general-vehicle-oriented coordinated timing plan to accommodate bus-service characteristics [34], as depicted in Figure 1. However, when passive TSP is applied to an arterial with near-side stops, additional factors must be considered because of dwell-time variability. Moreover, negative impacts on side-street traffic have long been one of the major issues associated with TSP. In this study, we attempt to deal with these issues.

2.1. Dwell Time Variability at Near-Side Stop. The dwell time and its variance as constraints on passive TSP have been considered in most previous studies [18, 21, 22]. The bus trajectory using a near-side stop is portrayed in Figure 2. In Figure 2(a), the dwell time has two components: number 1 denotes the boarding and alighting time, which the bus must always spend at the stop, and number 2 denotes the waiting time at the traffic signal after boarding and alighting, which varies with the end instant of number 1. A near-side stop has the highest dwell-time variability, which can reduce the TSP effect [35]. The action of this variability over a chain of multiple stops means that each bus can be considered to arrive at the stop randomly. Therefore, the various arrival instants of two-way buses at stops must be considered to increase the TSP effect while applying the TSP to near-side stops. Considering this situation, a previous study designed a TSP model using number 1 and number 2 [23]. However, STEP BAND [23] used an average value for the passenger boarding and alighting time, which is actually variable over time because of variations in passenger demand. By contrast, this study uses a normally distributed stochastic passenger boarding and alighting time to consider this variability.

In Figure 2(b), the effect of a bus bay is considered: number 1 denotes the time the bus waits to use the bus bay, which depends on the bay's capacity and the degree of bus bunching. This is important because the bus departure instant at the stop depends on whether the bus bay was used. Therefore, in a previous study, an upper bound of the bus bandwidth was set so that the storage capacity of the bus stop was not exceeded [22]. However, the actual bus arrived at the stop in a manner different from the plan owing to various road environmental factors. Thus, in calculating the dwell time, the possibility of failure to use bus bays should be considered; it will depend on the bus-stop capacity and the average number of bus arrivals per cycle length for each stop.

In this study, these factors were considered for optimizing the combination between subsystems after maximizing the two-way bandwidth in the stop units. In summary, the waiting time at the stop for each bus was calculated by random bus arrival time at the stop based on dwell time following normal distribution. Thus, the combination of each subsystem can be

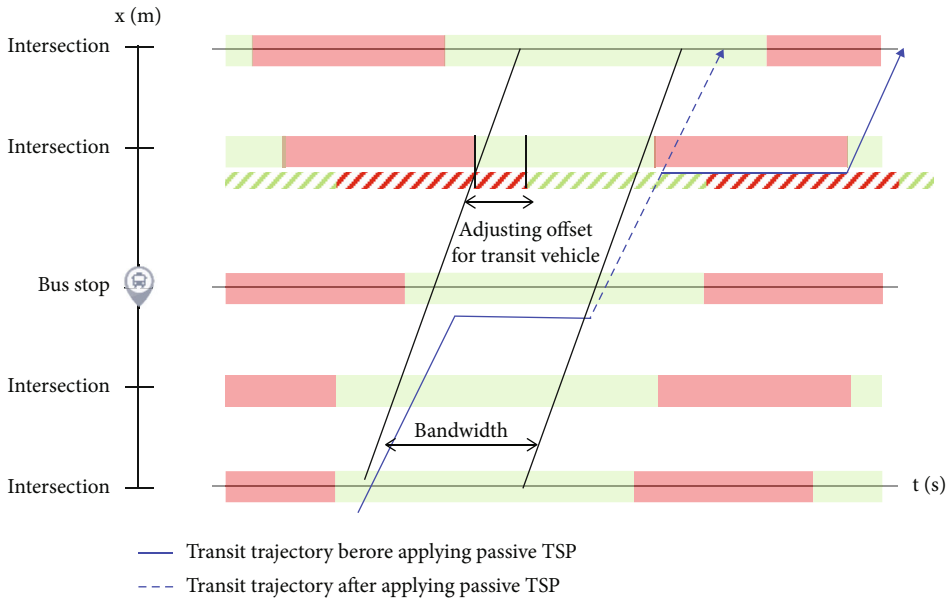

Figure 1: Transit-vehicle trajectory before and after application of simple passive transit-signal priority (TSP).

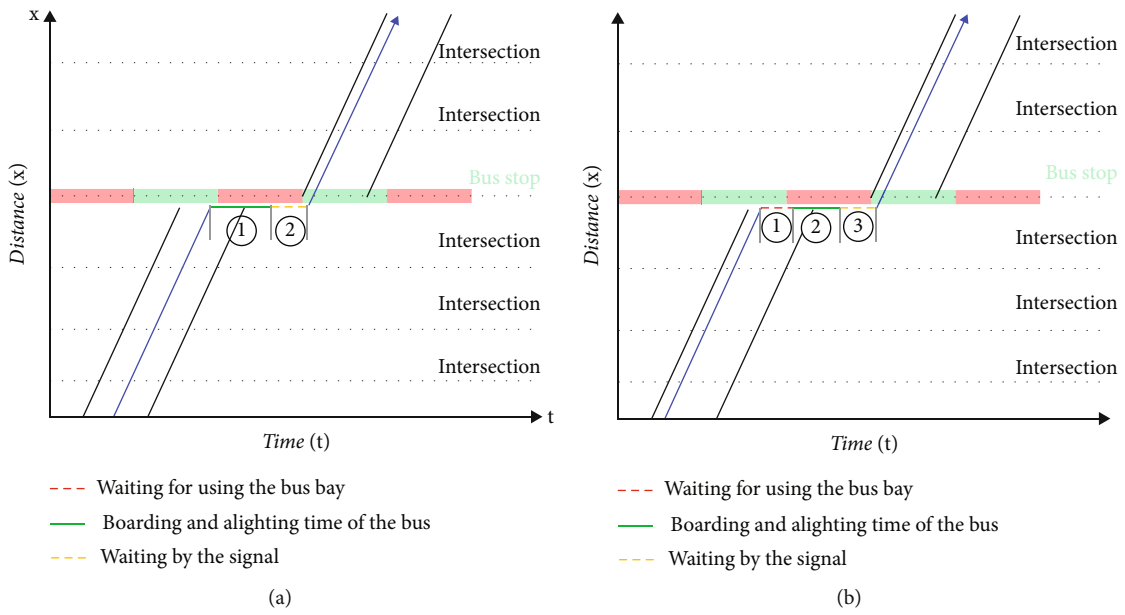

Figure 2: Bus trajectories at a near-side stop (a) without and (b) with a bus bay waiting.

optimized to minimize the total bus stop waiting time of two-way buses.

2.2. Other Road Users. In typical studies, a passive TSP is applied to an artery, and a model is developed to ensure the progression of both general and transit vehicles on the main road [17, 20, 23]. However, side-street users have rarely been considered; one exception is the work of Jeong and Kim [16], who maintained the existing cycle length and green split to satisfy the desired green times of other road users. In fact, if there is an intersection with heavy traffic volume on a side street or main arterial intersecting the transit corridor, the altered offset can have a negative impact. Therefore, the transit corridor has an "influential area" that will be affected by the introduction of TSP. We use our proposed model that was to perform signal adjustment and optimization in the entire influence area after optimizing the signal of the transit corridor. Based on the network, it could be used to calculate a signal plan that benefits the transit vehicle as well as the general vehicle.

3. Methodology

This paper proposes an integrated TSP system with a median-exclusive bus lane, assuming buses use near-side bus stops and

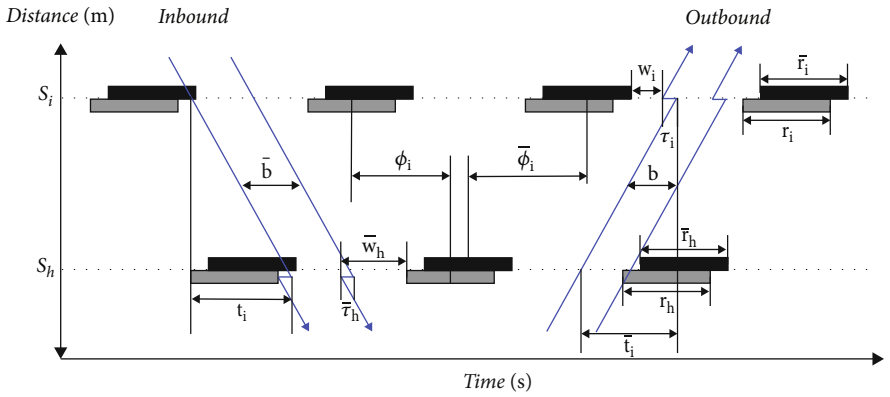

Figure 3: Time–space diagram for MAXBAND (symbols defined in Table 1).

Table 1: Symbols and parameters.

Notation	Description
$b/\bar{b}$	Outbound/inbound bandwidth [cycles]
$r_i\bar{r}_i/$	Outbound/inbound red time at s_i [cycles]
$w_i\bar{w}_i/$	Time from right/left side of the red at S_i to the left/right edge of the outbound/inbound green band [cycles]
$t_i/\bar{t}_i$	Travel time from s_i to s_h outbound/s_h to S_i inbound [cycles], $t_i = t(i, i+1)$
$\varnothing_i/\overline{\varnothing}_i$	Time from center of an outbound/inbound red at s_h to center of particular outbound/inbound red at s_i [cycles]
$\tau_i/\bar{\tau}_i$	Queue-clearance time, an advance of outbound/inbound bandwidth upon leaving s_i [cycles]
$l_i/\bar{l}_i$	Time allocated for outbound/inbound left turn green at s_i [cycles]
$\delta_i, \bar{\delta}_i$	Phase sequence of s_i, 0–1 variables
k	Target ratio of inbound to outbound bandwidth
z	Signal frequency, or the inverse of cycle length [cycles/s]
T_1/T_2	Lower and upper limits on cycle length [s]
$d_i/\bar{d}_i$	Distance between s_h and s_i outbound/inbound [meters], $d_i = d(i, i+1)$
$e_i, f_i/\bar{e}_i, \bar{f}_i$	Lower and upper limits on outbound/inbound speed [m/s]
$(1/h_i), (1/q_i)/(1/\bar{h}_i), (1/\bar{q}_i)$	Lower and upper limits on variation in outbound/inbound reciprocal speed $[\text{m/s}]^{-1}$

share the same signals with general vehicles. First, the sum of the two-way bandwidth is maximized in units of stops based on MAXBAND LP2 to find optimum internal-offset combination. Second, the external offset, a combination of several subsystems, is optimized to minimize the waiting time of the bus at the stop. Finally, we optimize the signals at intersections or arterial roads affected by the TSP.

3.1. Maximizing Two-Way Bandwidth by Bus Stop

3.1.1. MAXBAND LP2. MAXBAND LP2 model is a two-way arterial with a fixed number of signals. The cycle length and offsets of this model are also optimized to maximize the sum of the outbound and inbound bandwidths [36]. The two-way bandwidth between the two signals is illustrated in Figure 3. (For notation, see Table 1).

The problem of maximizing the sum of the two-way bandwidths (illustrated in Figure 3) can be expressed as follows:

$$\text{Max}\left(b + k\bar{b}\right)\left(\text{find } b, \bar{b}, z, w_i, \bar{w}_i, m_i, t_i, \bar{t}_i, \delta_i, \bar{\delta}_i\right), \tag{1}$$

$$(1/T_2) \le z \le \left(\frac{1}{T_1}\right), \tag{2}$$

$$w_i + b \le 1 - r_i \quad \forall i = 1, \cdots, n, \tag{3}$$

$$\bar{w}_i + \bar{b} \le 1 - \bar{r}_i \quad \forall i = 1, \cdots, n, \tag{4}$$

$$w_i + \bar{w}_i - w_{i+1} - \bar{w}_{i+1} + t_i + \bar{t}_i + \delta_i l_i - \bar{\delta}_i \bar{l}_i - \delta_{i+1} l_{i+1}, + \bar{\delta}_{i+1} \bar{l}_{i+1} - m_i = r_{i+1} - r_i + \bar{\tau}_i + \tau_{i+1} \quad \forall i = 1, \cdots, n-1, \tag{5}$$

$$(d_i f_i) z \le t_i \le \left(\frac{d_i}{e_i}\right) z \quad \forall i = 1, \cdots, n-1, \tag{6}$$

$$\left(\frac{\bar{d}_i}{\bar{f}_i}\right) z \le \bar{t}_i \le \left(\frac{\bar{d}_i}{\bar{e}_i}\right) z \quad \forall i = 1, \cdots, n-1, \tag{7}$$

$$\left(\frac{d_i}{h_i}\right) z \le \left(\frac{d_i}{d_{i+1}}\right) t_{i+1} - t_i \le \left(\frac{d_i}{q_i}\right) z \quad \forall i = 1, \cdots, n-2, \tag{8}$$

$$\left(\frac{\bar{d}_i}{\bar{h}_i}\right) z \le \left(\frac{\bar{d}_i}{\bar{d}_{i+1}}\right) \bar{t}_{i+1} - \bar{t}_i \le \left(\frac{\bar{d}_i}{\bar{q}_i}\right) z \quad \forall i = 1, \cdots, n-2, \tag{9}$$

$$b, \bar{b}, z, w_i, \bar{w}_i, t_i, \bar{t}_i \ge 0, \tag{10}$$

$$m_i : \text{integer}, \tag{11}$$

$$\delta_i, \bar{\delta}_i : \text{binary}. \tag{12}$$

The objective function maximized by MAXBAND LP2 is the sum of the two-way bandwidths; the scalar decision variables $b, \bar{b}, z, w_i, \bar{w}_i, m_i, t_i, \bar{t}_i, \delta_i, \bar{\delta}_i$ are calculated according to the objective function. Equation (2) limits the range of feasible cycle length, while Equations (3) and (4) express the constraints on the two-way bandwidth. Equation (5) limits the integer variables $\varnothing(h, i)$ and $\overline{\varnothing}(h, i)$. Equations (6) and (7) represent the constraints on the two-way travel speeds, and Equations (8) and (9) are constraints on their variation. Equation (10) imposes nonnegativity constraints, Equation (11) imposes an integer constraint, and Equation (12) imposes a constraint on the phase sequence.

3.1.2. STEP BAND. STEP BAND maximizes the two-way bandwidth in units of stops based on MAXBAND LP2 [23]. The subsystem can be divided into stops, considering the bus halts at the stop. Dai et al. [21] classified intersections according to bus-stop locations between adjacent intersections. However, this study targets the near-side stop with the signal; the subsystem sets the outbound direction as a weighted direction and ranges from the upstream stop to the intersection situated immediately before the downstream stop in the outbound direction. All transportation using the subsystem bandwidth can pass from the upstream stop to the downstream stop without halting. Thus, the lower and upper limits of the outbound/inbound travel times given in Equations (6) and (7) can be converted to a free flow speed. Consequently, the constraints described in Equations (8) and (9) are excluded from the STEP BAND. Since the two-way bandwidth is maximized in units of stops based on the outbound direction, the bus traveling in the outbound direction can utilize the red time at the stop for passenger boarding and alighting. However, in the inbound direction, the red time of the downstream stop cannot be utilized for this purpose, because the inbound bandwidth is maximized from the intersection directly after the upstream stop toward the downstream stop. Therefore, the inbound bandwidth is conditionally expanded, considering slack to be green. Furthermore, the last subsystem of the analysis section ranges from the upstream to the downstream stops based on the outbound direction, resulting in the same phenomenon as in the inbound direction. Thus, the outbound bandwidth of the last subsystem is also extended conditionally. The outbound and inbound bandwidths $(eb, \overline{eb})$ that are conditionally extended by STEP BAND in units of stops are illustrated in Figure 4.

3.2. Optimizing Subsystem Combination to Minimize Waiting Time at Stops. The constraints of STEP BAND optimizing the signals within the subsystem have been described above. In addition, adjacent subsystems should be combined to ensure a continuous flow of buses. Although Hao et al. [14] divided a long arterial into subgroups for efficient progression, this only optimized signals within each subgroup. Dai et al. [21] and Kim et al. [22] considered a combination of adjacent groups in the constraint, but all buses exhibited distinct arrival instants at stops within the cycle length owing to environmental factors. Han et al. [23] optimized system combinations assuming a uniform bus distribution, but an actual bus shows a random arrival distribution due to variability in dwell time and waiting for signals. The present study seeks to overcome the limitation in combination and optimization between subsystems due to the random arrival distribution of each bus. (For notation, see Table 2 and Figure 5.)

The combination of subsystems influences the waiting time of the bus at the stop because each subsystem is divided into stops. Therefore, the two-way bus waiting time experienced at the stops is considered when solving the problem of combination optimization in this study. We optimize the combination of subsystems using an external offset, which represents the deviation in the outbound-bandwidth start time for each upstream stop in the case of two adjacent subsystems.

Bus arrival time is affected by traffic condition, service headways, and user fraction [37]. To consider these factors, we assume first that we know when the buses enter the network (t_1 and t_2 in Figure 6). Extensive studies have confirmed that the arrival distribution of buses follows a normal, log normal, or gamma distribution [38–40]. Because this study deals with the near-side stop, which has the highest uncertainty in bus dwell time, and a stochastic arrival-time distribution based on a normally distributed stochastic dwell time has been adopted [30]. Each bus proceeds to a stop depending on whether a red light is shown after the boarding and alighting time at the near-side stop. A departure distribution of each bus is generated by taking k samples of bus departures based on the normally distributed dwell time. This study also assumes that all buses always use the full bandwidth. Therefore, the departure distribution at the upstream stop becomes the arrival distribution at the downstream stop. From the second stop, the bus-stop waiting time is calculated based on the boarding and alighting time following the normal distribution, the bus-bay availability, and the bandwidth availability. The passenger boarding and alighting time is extracted k times for each external offset to generate candidates for the optimal external offset, i.e., the offset for which the waiting time of the two-way bus is minimized in the situation where dwell time is variable.

The problem of combination optimization between subsystems can be expressed as follows:

Step 1.

$$D_{n,\theta} = D_n + i, \quad \forall i = 0, \cdots, C_n - 1, \tag{13}$$

$$\theta_n = D_{n+1} - D_{n,\theta}, \quad \forall i = 0, \cdots, C_n - 1, \tag{14}$$

$$\mathrm{WT}_{n+1,\theta,j,k} = \begin{cases} \left(S_{n+1,\theta,j-LA,k} + \mathrm{TWT}_{n+1,\theta,j-LA,k} - \mathrm{WT}_{n+1,\theta,j-LA,k}\right) - A_{n+1,\theta,j,k}, \\ \text{if } \left(\mathrm{LA}_{n+1} \le j\right), \left(S_{n+1,\theta,j-LA,k} + \mathrm{TWT}_{n+1,\theta,j-LA,k} - \mathrm{WT}_{n+1,\theta,j-LA,k} - A_{n+1,\theta,j,k} > 0\right) \\ 0, \text{ otherwise,} \end{cases} \tag{15}$$

$$S_{n+1,\theta,j,k} = A_{n+1,\theta,j,k} + \mathrm{DW}_{n+1,j,k} + \mathrm{WT}_{n+1,\theta,j,k}, \quad \forall i = 0, \cdots, C_n - 1, \tag{16}$$

$$\mathrm{TWT}_{n+1,\theta,j,k} = \begin{cases} \mathrm{WT}_{n+1,\theta,j,k}, \text{if } D_{n+1} \le S_{n+1,\theta,j,k} \le D_{n+1} + B_{n+1}, \\ D_{n+1} + C_{n+1} - S_{n+1,\theta,j,k} + \mathrm{WT}_{n+1,\theta,j,k}, \text{otherwise,} \end{cases} \tag{17}$$

$$\forall j = 0, \cdots, N_n - 1, \tag{18}$$

$$S\mathrm{TWT}_{n+1,\theta} = \sum_j \sum_k \mathrm{TWT}_{n+1,\theta,j,k}, \quad \forall i = 0, \cdots, C_n - 1. \tag{19}$$

Step 2.

$$\bar{D}_{n,\theta} = \bar{D}_n + i, \quad \forall i = 0, \cdots, C_n - 1, \tag{20}$$

$$\theta_n = D_{n+1} - D_{n,\theta}, \forall i = 0, \cdots, C_n - 1, \tag{21}$$

$$\overline{\mathrm{WT}}_{n+1,\theta,j,k} = \begin{cases} \left(\bar{S}_{n+1,\theta,j-\mathrm{LA},k} + \overline{\mathrm{TWT}}_{n+1,\theta,j-LA,k} - \overline{\mathrm{WT}}_{n+1,\theta,j-LA,k}\right) - \bar{A}_{n+1,\theta,j,k}, \\ \text{if } \left(\overline{\mathrm{LA}}_{n+1} \le j\right), \left(\bar{S}_{n+1,\theta,j-LA,k} + \overline{\mathrm{TWT}}_{n+1,\theta,j-LA,k} - \overline{\mathrm{WT}}_{n+1,\theta,j-LA,k} - \bar{A}_{n+1,\theta,j,k} > 0\right) \\ 0, \qquad \text{otherwise,} \end{cases} \tag{22}$$

$$\bar{S}_{n+1,\theta,j,k} = \bar{A}_{n+1,\theta,j,k} + \overline{\mathrm{DW}}_{n+1,j,k} + \overline{\mathrm{WT}}_{n+1,\theta,j,k}, \quad \forall i = 0, \cdots, C_n - 1, \tag{23}$$

$$\overline{\mathrm{TWT}}_{n+1,\theta,j,k} = \begin{cases} \overline{\mathrm{WT}}_{n+1,\theta,j,k}, & \text{if } \bar{D}_{n,\theta} \le \bar{S}_{n+1,\theta,j,k} \le \bar{D}_{n,\theta} + B_n, \\ \bar{D}_{n,\theta} + C_n - \bar{S}_{n+1,\theta,j,k} + \overline{\mathrm{WT}}_{n+1,\theta,j,k}, & \text{otherwise,} \end{cases} \tag{24}$$

$$\forall j = 0, \cdots, \bar{N}_n - 1, \tag{25}$$

$$\overline{S\mathrm{TWT}}_{n+1,\theta} = \sum_j \sum_k \overline{\mathrm{TWT}}_{n+1,\theta,j,k}, \quad \forall i = 0, \cdots, C_n - 1. \tag{26}$$

Step 3.

$$\mathrm{OP}n = \theta \text{ when minimize } \left(\mathrm{STWT}_{n+1,\theta} + \overline{\mathrm{STWT}}_{n+1,\theta}\right). \tag{27}$$

The optimal external offset required for minimizing the bus-waiting time at the stop can be determined by these three steps. Additionally, the outbound upstream subsystem is moved up to the cycle length every second to calculate the waiting time for using the downstream bandwidth of each bus with an external offset.

In Step 1, the waiting time of the outbound bus for each external offset is considered. Equation (13) represents the starting point of the upstream bandwidth, which varies with the movement of the upstream subsystem every second. Based on this equation, an external offset is obtained using Equation (14). The waiting time if the bus bay is not used is calculated in Equation (15). Based on the bus-bay capacity

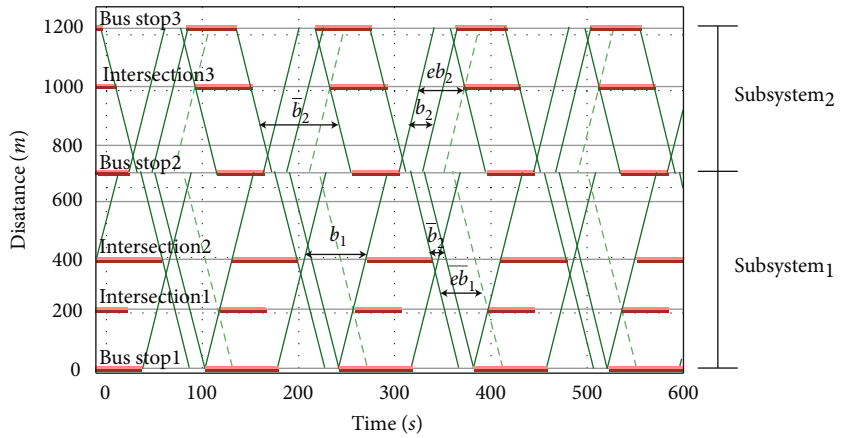

Figure 4: Time–space diagram for STEP BAND (symbols defined in Table 1).

Table 2: Additional notation.

Notation	Description
θ_n	External offset between subsystem $_n$ and subsystem $_{n+1}$ [s]
C_n	n^{th} stop cycle length [s]
$D_n/\bar{D}_n$	Outbound/inbound bandwidth starting point at n^{th} stop [s]
$B_n/\bar{B}_n$	Outbound/inbound bandwidth of subsystem $_n$ maximized through STEP BAND [s]
$A_{n,\theta,j}/\bar{A}_{n,\theta,j}$	Time when j^{th} bus traveling on outbound/inbound arrives at n^{th} stop [s]
$DW_{n,j}/\overline{DW}_{n,j}$	Boarding and alighting time of outbound/inbound j^{th} bus at n^{th} stop [s]
$S_{n,\theta,j}/\bar{S}_{n,\theta,j}$	End-point of dwell time of outbound/inbound j^{th} bus at n^{th} stop [s]
$N_n/\overline{N}_n$	Average number of outbound/inbound buses using n^{th} stop [bus/cycle]
$LA_n/\overline{LA}_n$	Number of bus bays on outbound/inbound at n^{th} stop
$WT_{n,\theta,j}/\overline{WT}_{n,\theta,j}$	Waiting time of outbound/inbound j^{th} bus under failure to use the bus bay at n^{th} stop [s]
$TWT_{n,\theta,j}/\overline{TWT}_{n,\theta,j}$	Waiting time of outbound/inbound j^{th} bus at n^{th} stop [s]
$STWT_{n,\theta}/\overline{STWT}_{n,\theta}$	The sum of the waiting times of all buses in outbound/inbound using n^{th} stop at θ_n [s]
OP_n	Optimum external offset between subsystem $_n$ and subsystem $_{n+1}$ [s]

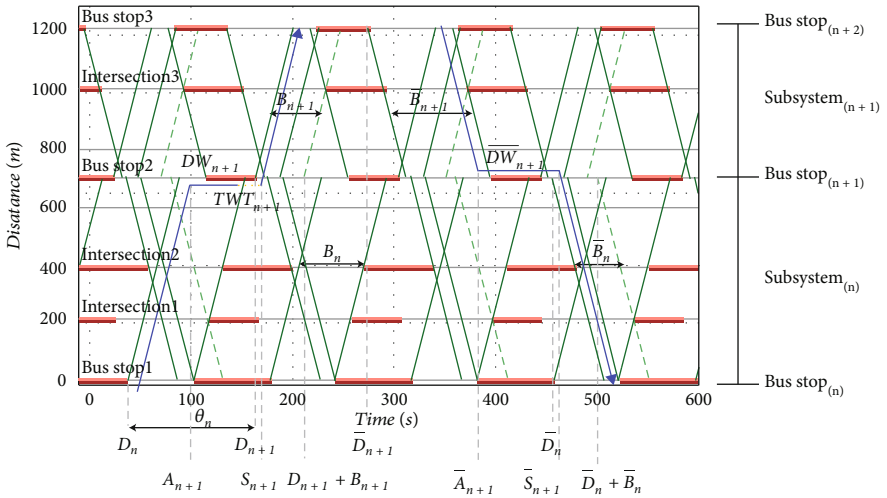

Figure 5: Variables used to optimize the combination between subsystems (symbols defined in Tables 2).

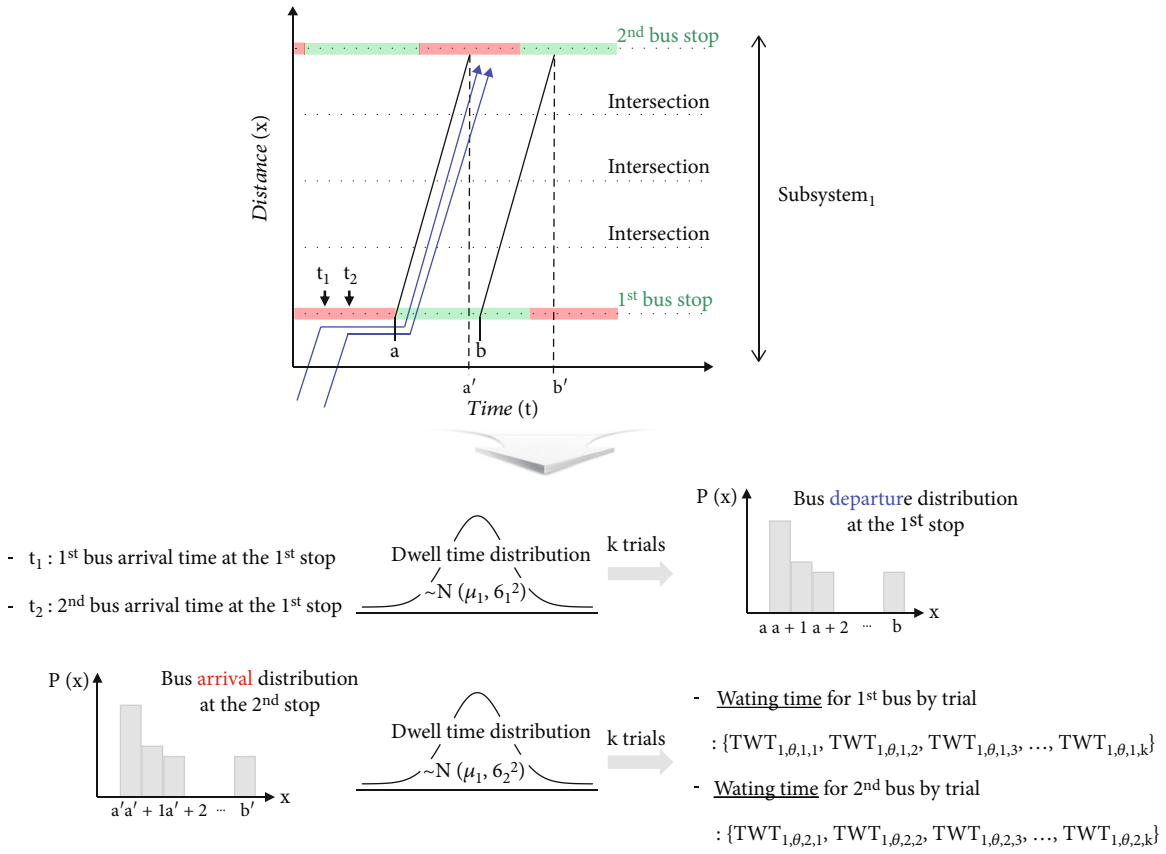

Figure 6: Bus-arrival distribution.

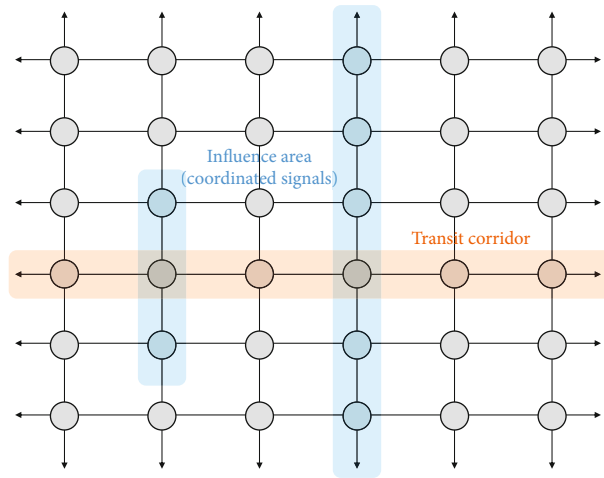

Figure 7: Adjacent intersections affected by transit-signal priority. Orange-shaded area: transit corridor; blue-shaded area: influence area.

and the bay-use time of the leading bus, the bay-use waiting time of the following bus is determined, depending on whether it actually uses the bus bay. Equation (16) expresses the end instant of the bus dwell time, which is determined by the time spent waiting for bus bay availability, the passenger boarding and alighting times, and the bus-arrival distribution. Equation (17) can be used to calculate the waiting time for each bus at the stop according to the availability of downstream-subsystem bandwidth at the end instant of the bus dwell time. Overall, the waiting time for each bus depends on failure to use the bus bay and on downstream bandwidth. Equation (18) gives the average number of buses arriving at the stop per cycle length, which is used to calculate the bus-bay capacity. Equation (18) is obtained by converting the

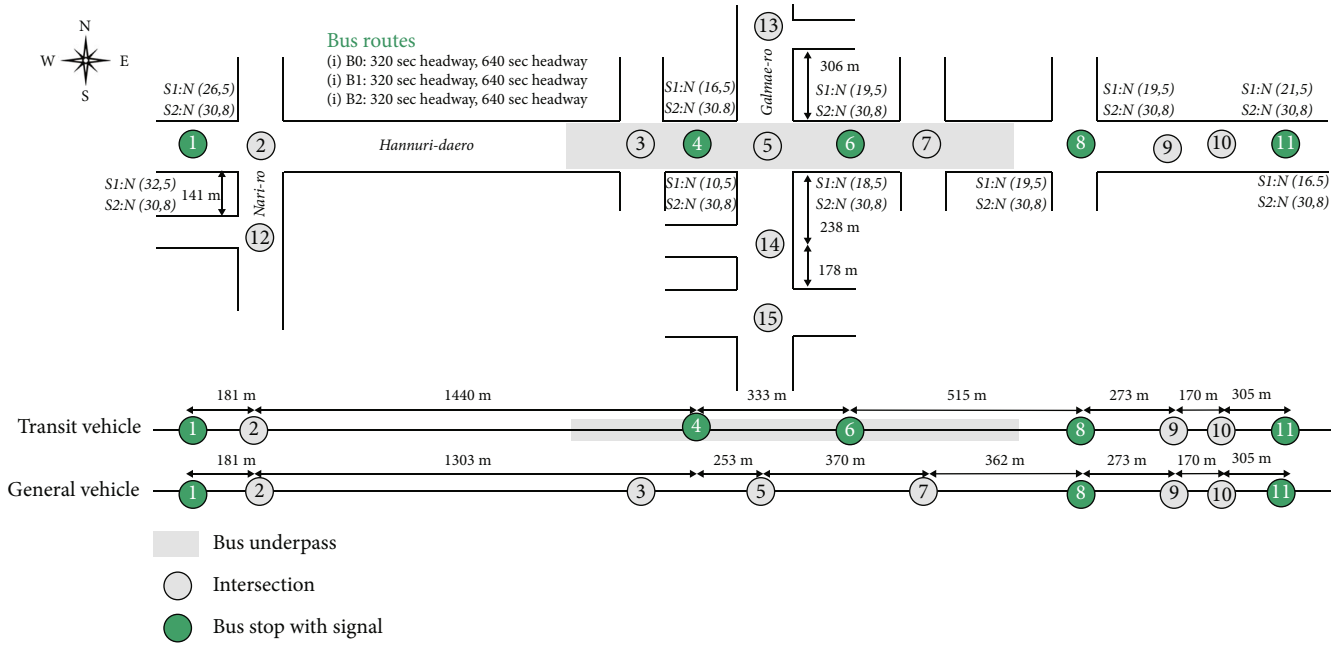

Figure 8: Location information of test site.

Table 3: Simulation scenario.

Dwell time Headway	Mean based on BMS-data average; standard deviation, 5 s	Mean, 30 s; standard deviation, 8 s
320 (s)	Scenario 1-1	Scenario 2-1
640 (s)	Scenario 1-2	Scenario 2-2

average number of buses arriving per hour into a cycle length unit and rounding it up. In addition, the boarding and alighting time of the bus at the stop was randomly extracted for k trials based on the normal distribution. Therefore, the processes expressed in Equations (15)–(17)are repeated by the number of trials k and the average number of buses $N_n/\bar{N}_n$ arriving at the stop per cycle length. The sum of the waiting time of all buses for each external offset is evaluated using Equation (19).

Step 2 calculates the waiting time for inbound buses under an external offset. Equation (20) represents the starting point of the inbound bandwidth according to the change in the external offset. Waiting time due to failure to use the bus bay is considered in Equation (22). Equation (24) gives the delay time of the j^{th} bus according to the availability of inbound bandwidth at the end of the dwell time computed in Equation (23). Based on the average number of buses in Equation (25) and k trials, Equation (26) calculates the sum of the waiting times of all inbound buses.

Finally, in Step 3, the optimal external offset is determined by considering the two-way bus waiting time for each external offset (Equation (27)). By following this process, buses can continuously travel across multiple subsystems. Moreover, the total waiting time at the stops is minimized for all the buses randomly arriving at each stop.

3.3. Optimizing Signals in the Influence Area. Other road users pose the greatest concern when applying TSP. Through the process proposed in this paper, general vehicles on the main street can drive uninterruptedly through several intersections between stops. However, the offset varies when passive TSP is applied to the arterial, thereby affecting side-street traffic. Most previous studies did not consider this effect, the impact of which may be severe if the arterial road to which TSP is applied intersects a main arterial road.

One strategy for mitigating such impacts is to optimize the signal-operation plan of the transit corridor, then adjust the relative offset based on the current signal-operation plan of the intersecting artery. As the signal-operation plan of TSP operation section changes, however, other adjacent roads may be affected by the changed traffic pattern. Therefore, an alternative strategy is to optimize the signal plan for influence areas, such as side-street intersections with heavy traffic volumes or major arterials crossing the transit corridor, as depicted in Figure 7.

Signal optimization of the influential area was calculated was Synchro Studio 7 [41], based on the following rules:

(i) All the optimized signals on the transit corridor are fixed

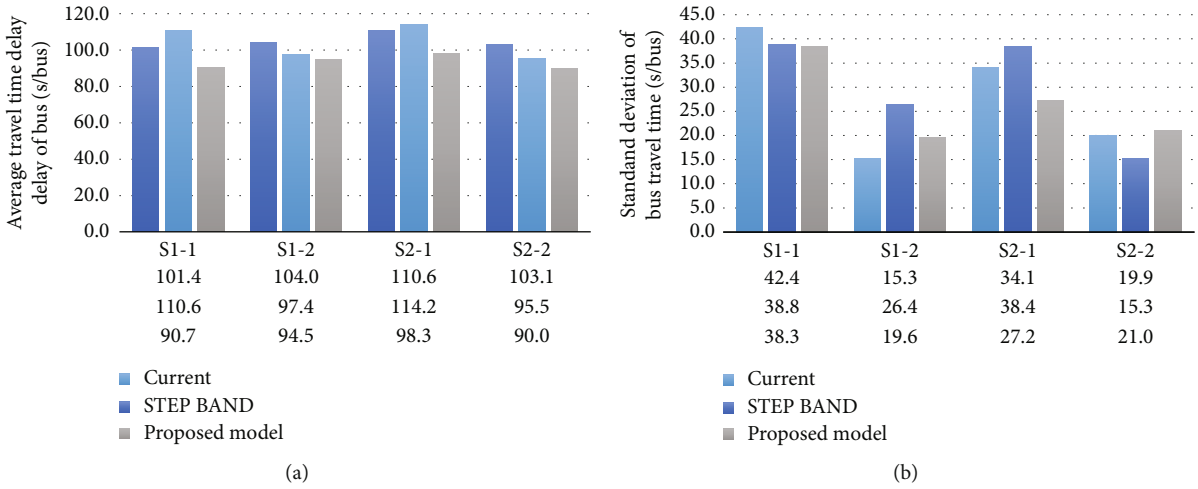

Figure 9: Bus travel-time delays (s/veh) for three models in four scenarios: (a) averages and (b) standard deviations.

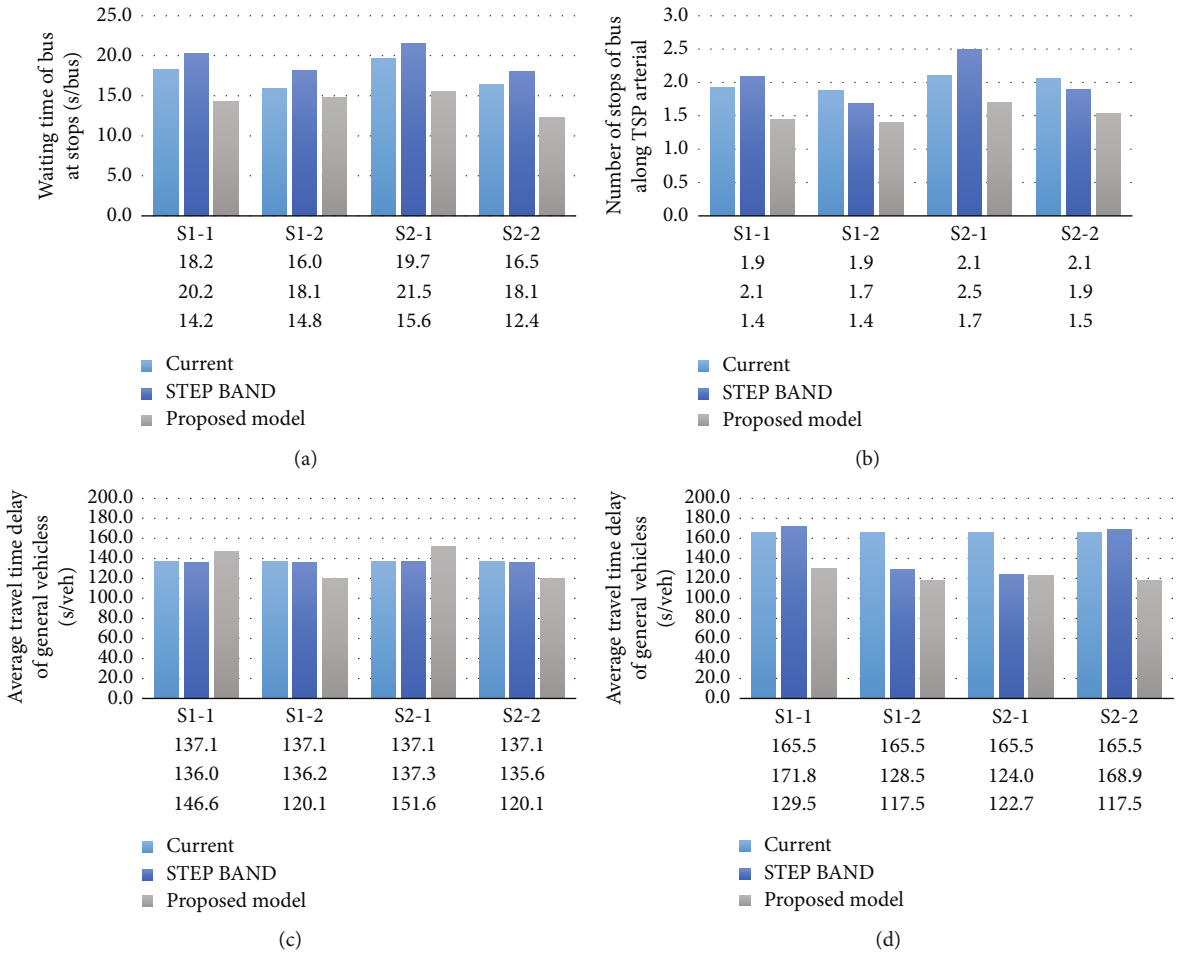

Figure 10: Performance comparison of three models in four scenarios: (a) average waiting times of bus at stops (s/bus); (b) number of stops of bus along transit corridor; (c–d) average travel time delays of general vehicles (s/veh) (c) on transit corridor and (d) on arterial in influence area.

Table 4: Intersection delays (s/veh).

Inter section	Scenario											
	Current	S1-1 STEP BAND	Proposed model	Current	S1-2 STEP BAND	Proposed model	Current	S2-1 STEP BAND	Proposed model	Current	S2-1 STEP BAND	Proposed model
1	3.9	4.2	6.5	3.4	3.4	5.9	3.8	3.8	6.2	3.4	3.4	5.9
2	24.6	24.9	28.7	25.0	24.9	29.2	24.9	24.7	29.6	25.0	24.4	29.3
3	35.3	40.1	29.3	34.7	27.2	21.5	39.6	40.3	32.7	34.6	36.8	27.4
4	13.8	14.6	10.8	13.8	14.0	10.9	13.8	14.0	10.8	13.8	13.8	10.9
5	26.9	31.1	23.6	26.9	28.3	23.1	26.9	27.9	24.8	26.9	28.6	23.1
6	24.1	26.3	20.6	21.5	15.8	16.8	24.2	22.9	20.2	21.5	21.6	19.5
7	31.9	32.9	28.3	31.9	40.5	26.9	31.9	42.9	25.8	31.9	43.2	26.9
8	23.2	15.0	14.1	23.3	14.9	13.7	23.3	18.1	14.0	23.4	17.7	13.4
9	16.2	8.9	5.8	16.6	2.5	8.8	15.9	1.9	6.3	16.6	1.6	8.6
10	5.0	11.0	10.1	5.2	10.1	11.6	4.9	4.9	11.2	5.1	4.8	11.6
11	5.7	16.8	12.5	5.1	6.2	18.8	5.9	9.1	19.2	5.1	8.8	19.2
12	10.4	10.2	9.8	10.4	10.4	9.8	10.3	10.4	9.8	10.4	10.3	9.8
13	16.0	18.8	18.0	16.0	15.6	18.4	16.0	15.6	17.4	16.0	15.7	18.4
14	11.7	5.6	5.1	11.7	10.6	5.0	11.7	10.8	3.9	11.7	11.7	5.0
15	87.4	77.4	64.9	87.4	71.3	63.0	87.4	74.0	62.9	87.4	85.3	63.0

Table 5: Network delays.

Scenario		Vehicle delay (s/veh)	Improvement Rate (%)	Person delay (s/per)	Improvement Rate (%)
S1-1	Current	28.3	—	19.0	—
	STEP BAND	27.0	4.5%	20.4	-7.2%
	Proposed model	23.4	17.3%	17.3	9.2%
S1-2	Current	28.4	—	18.7	—
	STEP BAND	26.0	8.8%	16.7	10.9%
	Proposed model	23.6	17.1%	16.7	10.9%
S2-1	Current	28.3	—	19.8	—
	STEP BAND	26.6	6.2%	20.6	-4.2%
	Proposed model	23.4	17.4%	17.8	10.0%
S2-2	Current	28.4	—	18.7	—
	STEP BAND	28.6	-0.4%	20.4	-9.2%
	Proposed model	23.6	17.0%	17.3	7.5%

(ii) The influence area uses the same cycle length as the transit corridor to continuously provide the same effect

(iii) Overlap is allowed to use the green time efficiently according to traffic level upon optimizing green splits and phase sequences

(iv) The network offset is the objective function optimized to minimize network delay

4. Test Site and Experimental Design

Certain roads in Sejong, Korea (Figure 8) were chosen as test sites and simulated to evaluate the effectiveness of the proposed methodology for real-world applications. The simulation network comprised fifteen intersections with five near-side stops in each direction (except for the westbound of stop 4, which is a far-side shape). The transit corridor was Hannuri-daero; some of its sections have a bus underpass, so that general vehicles and buses ply on distinct driving

sections. The bus travels on a median-exclusive bus lane; both buses and general vehicles traveling through Hannuri-daero use the same signals. Certain sections of Hannuri-daero where only general vehicles pass, together with the major intersections with Nari-ro and Galmae-ro, were defined as influence areas. For each arterial, all intersections were controlled using the pretimed strategy, and they share the same cycle length.

To apply the proposed model to various situations, several scenarios were organized according to the bus dwell times and volume, as shown in Table 3. In scenario 1-1, dwell time at a bus stop follows a normal distribution with a mean based on the average value of bus-management-system (BMS) data and a standard deviation of 5 s; all buses have a headway of 320 s. The headway is set to 640 s in scenario 1-2. In scenario 2-1, the dwell time of each bus stop follows a normal distribution with a mean of 30 s and standard deviation of 8 s; all buses have a headway of 320 s. The headway is set to 640 s in scenario 2-2. A current signal system and STEP BAND [23] were compared with the proposed methodology for equal cycle lengths of 160 s. Depending on the bus volume, approximately 17 and 34 buses were operated in each direction per hour, and approximately 23 cycle lengths were repeated. As stops 4 and 6 contain only one bus bay in each direction, a number of buses may experience waiting to use the bus bay at these stops. The optimal signal coordination plans were computed using Python with mixed-integer linear programming and SYNCHRO; the simulation experiments were conducted using VISSIM. In addition, each measure of effectiveness was calculated through the VISSIM and COM interface.

5. Result

This study adopted the average travel-time delay, average bus-stop waiting time, number of stops along an arterial, intersection delay, and network delay as measures of effectiveness to assess the performance of the proposed model on the network. In each scenario, the proposed model was compared with a current signal operation method and STEP BAND [23].

The average travel-time delay of a bus is vital for evaluating the speed of bus operation. As shown in Figure 9(a), the delays under the proposed model were shorter than those under the current signal and STEP BAND in all scenarios; compared to STEP BAND, they decreased by 18.1%, 3.0%, 13.9%, and 5.8% for scenarios 1-1, 1-2, 2-1, and 2-2, respectively. The standard deviations of the bus travel-time delays were similar to or slightly lesser than those obtained with STEP BAND (Figure 9(b)).

As depicted in Figure 10(a), the proposed model effectively reduced the bus waiting time for stops where all buses experienced dwell time variance. As shown in Figure 10(b), the current signal operation method and STEP BAND yielded a higher number of halts, including those at intersections and while waiting for the signal at the end of the dwell time. Considering scenario 1 as an example, the current system generated 1.9 halts, whereas the proposed model generated 1.4, a reduction of 26%. As indicated in Figure 10(c), the application of the proposed model showed similar the average travel-time delays of general vehicles on the transit corridor. Moreover, compared to the current signal operation method, the signal operation of the arterial in the influence area was improved by 22%, 29%, 26%, and 29% for each scenario, as depicted in Figure 10(d).

The proposed method outperformed the current signal operation method and STEP BAND at intersections, as indicated in Table 4. Although certain intersections exhibited slightly increased average delays per vehicle, most saw improvements. In summary, as shown from a network perspective in Table 5, the proposed model reduced vehicle delays by approximately 17% over the current system; person delays improved by approximately 9.2%, 10.9%, 10.0%, and 7.5% for each scenario, respectively.

6. Conclusions

This paper proposed an integrated traffic-signal system for a transit corridor with near-side stops and an influence area. The proposed model included a transit-oriented base signal plan along the transit corridor and base signals to minimize delays for general vehicles in the influence region. The base signal plan was formulated in three steps: first, the subsystem was divided into designated bus stops, and the two-way bandwidth was maximized based on STEP BAND. Thereafter, the combination of adjacent subsystems was optimized to minimize the waiting time of the two-way buses at each stop. In this step, random bus arrivals were generated by stochastic dwell time, and the capacity of the bus stop was also considered. Finally, the signals in the influence area, including those at intersections and arterials affected by TSP, were optimized using the green split and phase sequence, including an offset that minimized the network delay based on the same cycle length of the transit corridor.

A case study showed that, compared with the current signal operation method and STEP BAND, the proposed model could significantly enhance the operation of both buses and general vehicles in terms of average bus-travel-time delays and their standard deviation, average waiting times at stops, number of halts, and average travel delays of general vehicles in the transit corridor and the influence area. The proposed model can yield positive results for both vehicles and persons in terms of networks.

Various extensions of the proposed model are possible. First, the influence area could be defined more broadly than simply as the major intersections affected by TSP. As network delays may vary depending on the scope of the influence area, systematic conditions are required. Second, this study targeted an arterial road with TSP; however, the proposed model should be applied to a network with multiple bus routes. In the future, the simultaneous implementation of both passive and conditional-active TSP strategies should also be studied.

Data Availability

All the relevant data used to support the findings of the study are available within the article.

Conflicts of Interest

The authors declare that there is no conflict of interest regarding the publication of this paper.

Acknowledgments

This research was supported by a grant from the Development of S-BRT Priority Signal and Safety Management Technology Program funded by the Ministry of Land, Infrastructure, and Transport of Korea [grant number 22SBRT-C158062-03].

References

[1] W. D. Brooks, "Vehicular traffic control—designing arterial progressions using a digital computer," *IBM Document*, 1965.

[2] C. J. Messer, R. H. Whitson, C. L. Dudek, and E. J. Romano, "A variable-sequence multiphase progression optimization program," *Highway Res. Rec.*, vol. 445, pp. 24–33, 1973.

[3] J. D. C. Little and M. D. Kelson, *Optimal Signal Timing for Arterial Signal Systems*, vol. 1, Summary Report, 1980, FHWA/RD-80/082.

[4] E. C. P. Chang, S. L. Cohen, C. Liu, N. A. Chaudhary, and C. Messer, "MAXBAND-86: program for optimizing left-turn phase sequence in multi-arterial closed networks," *Transportation Research Record*, vol. 1181, pp. 61–67, 1988.

[5] N. H. Gartner, S. F. Assman, F. Lasaga, and D. L. Hou, "A multi-band approach to arterial traffic signal optimization," *Transportation Research Part B*, vol. 25, no. 1, pp. 55–74, 1991.

[6] Z. Tian and T. Urbanik, "System partition technique to improve signal coordination and traffic progression," *Journal of Transportation Engineering*, vol. 133, no. 2, pp. 119–128, 2007.

[7] L. T. Lin, L. W. Tung, and H. C. Ku, "Synchronized signal control model for maximizing progression along an arterial," *Journal of Transportation Engineering*, vol. 136, no. 8, pp. 727–735, 2010.

[8] J. Q. Li, "Bandwidth synchronization under progression time uncertainty," *IEEE Transactions on Intelligent Transportation Systems*, vol. 15, no. 2, pp. 749–759, 2014.

[9] X. Yang, Y. Cheng, and G.-L. Chang, "A multi-path progression model for synchronization of arterial traffic signals," *Transportation Research Part C*, vol. 53, pp. 93–111, 2015.

[10] C. Zhang, Y. Xie, N. H. Gartner, C. Stamatiadis, and T. Arsava, "AM-Band: an asymmetrical multi-band model for arterial traffic signal coordination," *Transportation Research Part C*, vol. 58, pp. 515–531, 2015.

[11] B. Ye, W. Wu, and W. Mao, "A two-way arterial signal coordination method with queueing process considered," *IEEE Transactions on Intelligent Transportation Systems*, vol. 16, no. 6, pp. 3440–3452, 2015.

[12] L. Zhang, Z. Song, X. Tang, and D. Wang, "Signal coordination models for long arterials and grid networks," *Transportation Research Part C*, vol. 71, pp. 215–230, 2016.

[13] X. Yang and Y. Cheng, "Development of signal optimization models for asymmetric two-leg continuous flow intersections," *Transportation Research Part C*, vol. 74, pp. 306–326, 2017.

[14] W. Hao, Y. Lin, Y. Cheng, and X. Yang, "Signal progression model for long arterial: intersection grouping and coordination," *IEEE Access*, vol. 6, pp. 30128–30136, 2018.

[15] W. Ma, K. L. Head, and Y. Feng, "Integrated optimization of transit priority operation at isolated intersections: a person-capacity-based approach," *Transportation Research Part C*, vol. 40, pp. 49–62, 2014.

[16] Y. Jeong and Y. Kim, "Tram passive signal priority strategy based on the MAXBAND model," *KSCE Journal of Civil Engineering*, vol. 18, no. 5, pp. 1518–1527, 2014.

[17] Y. Bai, J. Li, T. Li, L. Yang, and C. Lyu, "Traffic signal coordination for tramlines with passive priority strategy," *Mathematical Problems in Engineering*, vol. 2018, Article ID 6062878, 14 pages, 2018.

[18] K. Florek, "Arterial traffic signal coordination for general and public transport vehicles using dedicated lanes," *Journal of Transportation Engineering, Part A: Systems*, vol. 146, no. 7, p. 04020051, 2020.

[19] G. Y. Dai, H. Wang, and W. Wang, "A bandwidth approach to arterial signal optimisation with bus priority," *Transportmetrica A*, vol. 11, no. 7, pp. 579–602, 2015.

[20] W. Ma, L. Zou, K. An, N. H. Gartner, and M. Wang, "A partition-enabled multi-mode band approach to arterial traffic signal optimization," *IEEE Transactions on Intelligent Transportation Systems*, vol. 20, no. 1, pp. 313–322, 2019.

[21] G. Y. Dai, H. Wang, and W. Wang, "Signal optimization and coordination for bus progression based on MAXBAND," *KSCE Journal of Civil Engineering*, vol. 20, no. 2, pp. 890–898, 2016.

[22] H. Kim, Y. Cheng, and G.-L. Chang, "Variable signal progression bands for transit vehicles under dwell time uncertainty and traffic queues," *IEEE Transactions on Intelligent Transportation Systems*, vol. 20, no. 1, pp. 109–122, 2019.

[23] Y. Han, M. Kim, and Y. Kim, "Progression control model to enhance performance of transit signal priority," *IEEE Access*, vol. 10, pp. 14397–14408, 2022.

[24] H. R. Smith, B. Hemily, and M. Ivanovic, *Transit Signal Priority (TSP): A Planning and Implementation Handbook*, ITS America, Washington, DC, 2005.

[25] M. Garrow and R. Machemehl, "Development and evaluation of transit signal priority strategies," *Journal of Public Transportation*, vol. 2, no. 2, pp. 65–90, 1999.

[26] M. Zlatkovic, A. Stevanovic, P. T. Martin, and I. Tasic, "Evaluation of transit signal priority options for future bus rapid transit line in West Valley City, Utah," *Transportation Research Record*, vol. 2311, no. 1, pp. 176–185, 2012.

[27] Y. Lin, X. Yang, G.-L. Chang, and N. Zou, "Transit priority strategies for multiple routes under headway-based operations," *Transportation Research Record*, vol. 2356, no. 1, pp. 34–43, 2013.

[28] Z. Ye and M. Xu, "Decision model for resolving conflicting transit signal priority requests," *IEEE Transactions on Intelligent Transportation Systems*, vol. 18, no. 1, pp. 59–68, 2017.

[29] J. Shi, Y. Sun, P. Schonfeld, and J. Qi, "Joint optimization of tram timetables and signal timing adjustments at intersections," *Transportation Research Part C*, vol. 83, pp. 104–119, 2017.

[30] L. T. Truong, G. Currie, M. Wallace, C. De Gruyter, and K. An, "Coordinated transit signal priority model considering stochastic bus arrival time," *IEEE Transactions on Intelligent Transportation Systems*, vol. 20, no. 4, pp. 1269–1277, 2019.

[31] Z. Mei, Z. Tan, W. Zhang, and D. Wang, "Simulation analysis of traffic signal control and transit signal priority strategies

under arterial coordination conditions," *SIMULATION*, vol. 95, no. 1, pp. 51–64, 2019.

[32] H. Kim, Y. Cheng, and G.-L. Chang, "An arterial-based transit signal priority control system," *Transportation Research Record*, vol. 2672, no. 18, pp. 1–14, 2018.

[33] B. Moghimi and C. Kamga, "Models and technologies for smart, sustainable and safe transportation systems: transit signal priority in smart cities," *IntechOpen*, 2021.

[34] A. Skabardonis, "Control strategies for transit priority," *Transportation Research Record*, vol. 1727, no. 1, pp. 20–26, 2000.

[35] W. Kim and L. R. Rilett, "Improved transit signal priority system for networks with nearside bus stops," *Transportation Research Record*, vol. 1925, no. 1, pp. 205–214, 2005.

[36] J. D. C. Little, M. D. Kelson, and N. H. Gartner, "MAXBAND: a program for setting signals on arterials and triangular networks," *Transportation Research Record*, vol. 759, pp. 40–46, 1981.

[37] S. I. J. Chien, S. K. Daripally, and K. Kim, "Development of a probabilistic model to optimize disseminated real-time bus arrival information for pre-trip passengers," *Journal of Advanced Transportation*, vol. 41, no. 2, pp. 195–215, 2007.

[38] R. P. Guenthner and K. Hamat, "Distribution of bus transit on-time performance," *Transportation Research Record*, vol. 1202, pp. 1–8, 1988.

[39] D. Taş, N. Dellaert, T. Van Woensel, and T. De Kok, "Vehicle routing problem with stochastic travel times including soft time windows and service costs," *Computers & Operations Research*, vol. 40, no. 1, pp. 214–224, 2013.

[40] Q. Sun, S. Chien, D. Hu, and X. Chen, "Optimizing customized transit service considering stochastic bus arrival time," *Journal of Advanced Transportation*, vol. 2021, Article ID 3207025, 2021.

[41] D. Husch and J. Albeck, *Synchro studio 7 user guide*, Trafficware Ltd, 2006.